

Thermophysics of metal alkanooates

III. Heat capacities and thermodynamic properties of lithium and potassium propanoates^a

P. FRANZOSINI^b and EDGAR F. WESTRUM, JR.

*Department of Chemistry, University of Michigan,
Ann Arbor, Michigan 48109, U.S.A.*

(Received 23 May 1983; in revised form 11 July 1983)

At 298.15 K, the values of $C_{p,m}/R$, S_m°/R , $\{H_m^\circ - H_m^\circ(0)\}/R$, and $\{G_m^\circ - H_m^\circ(0)\}/RT$ are 15.58, 17.13, 2588.6 K, and -8.445 for $\text{CH}_3\text{CH}_2\text{CO}_2\text{Li}(\text{cr})$, and 17.30, 21.16, 3134.0 K, and -10.647 for $\text{CH}_3\text{CH}_2\text{CO}_2\text{K}(\text{cr})$. The energetics and shape of the (crystal III-to-crystal II) transition at $T_{\text{tr}} = 255$ K in the potassium compound are investigated. The lithium compound showed a (crystal II-to-crystal I) transition not far above 500 K, and fusion at 606.8 K. Relative trends in the Li, Na, and K salts are unexplained because of lack of structural information.

1. Introduction

Previous papers of the present series^(1,2) report the thermophysical behavior of the three lowest homologs of the sodium *n*-alkanoate family (methanoate, ethanoate, and propanoate). In order to investigate how changing the cation affects the molar heat capacity within a group of alkali alkanooates having a common anion, propanoates are now preferred to methanoates or ethanoates inasmuch as d.s.c. analysis shows⁽³⁾ that for both methanoates and ethanoates solid-state transitions (when present) are often very sluggish and, moreover, that there is a tendency to form vitreous phases (*e.g.* in lithium methanoate and ethanoate). This work concerns mainly the thermophysics of lithium and potassium propanoates from liquid-helium temperatures up to 350 K; some results obtained for the former salt in the superambient region are also included.

For subsequent discussion, it is convenient to summarize (in table 1) the pertinent information available in the literature.

2. Experimental

Lithium and potassium propanoates were prepared by reacting in turn Fluka puriss. Li_2CO_3 (in de-ionized water) and Fluka puriss. K_2CO_3 (in anhydrous methanol)

^a This research was supported in part by the Structural Chemistry and Chemical Thermodynamics Program of the Division of Chemistry of the National Science Foundation under Grant CHE-8007977. The preceding papers in this series are references 1 and 2.

^b Present address: Dipartimento di Chimica-Fisica, University of Pavia, Pavia, Italy.

with a slight excess (2 per cent) of Fluka puriss. p.a. (≥ 99.5 moles per cent; tested by g.c. at the origin) propanoic acid. Solid lithium propanoate was recovered by vacuum freeze-drying, and subsequently purified by dissolution in methanol and fractional precipitation with ethyl ether. Solid potassium propanoate was recovered by evaporation of the solvent and excess acid under reduced pressure in a Rotavapor device at about 330 K, and subsequently purified by recrystallization from (isopropanol + ethanol + methanol) (4,2,1 by volume). Both salts were dried after purification under vacuum at about 330 K to constant mass, and tested by d.s.c., which gave records fully agreeing with those reported in reference 3. The finely ground portions employed for the preparation of the samples were submitted to final drying at about 400 K for a few days before use.

The technique of computer-operated equilibrium adiabatic calorimetry in both cryogenic and superambient regions has been described previously.⁽¹⁾ The gold-plated copper calorimeter employed with the Mark X cryostat in the temperature range between the liquid-helium region and 350 K was loaded with 28.0860 g of $\text{CH}_3\text{CH}_2\text{CO}_2\text{Li}$ (0.3510 mol, calculated on the basis of the IUPAC 1973 relative atomic masses) and 37.7891 g of $\text{CH}_3\text{CH}_2\text{CO}_2\text{K}$ (0.3369 mol). The silver calorimeter employed with the Mark IX thermostat for the exploratory measurements in the superambient region was loaded with 21.3269 g of $\text{CH}_3\text{CH}_2\text{CO}_2\text{Li}$ (0.2665 mol). After loading, the air within the calorimeters was replaced with a few kPa (at 300 K) of helium, and buoyancy corrections were calculated.

3. Results

The experimental molar heat capacities obtained in the Mark X cryostat are listed in chronological order in table 2 and shown in figure 1 for lithium propanoate, and

TABLE 1. Phase changes of lithium and potassium propanoates as reported in previous literature

Salt	Phase change	T/K	$\Delta H_m/(R\text{ K})$	Method	Ref.
$\text{CH}_3\text{CH}_2\text{CO}_2\text{Li}$	trs ^a	538	—	visual	4
	fus ^b	602	—	visual	5
	fus	600 ± 1	—	d.s.c.	6
	trs	533 ± 2	400	d.s.c.	3
	fus(m) ^c	584	2140		
	fus	606.8	1910		
$\text{CH}_3\text{CH}_2\text{CO}_2\text{K}$	trs	341	—	visual	4
	trs	603	—		
	fus	639	—	visual	7
	fus	628	—	micr. ^d	8
	fus	631 ± 1	—	d.s.c.	6
	trs	258 ± 2	40	d.s.c.	3 ^e
	trs	352.5	210		
	fus	638.3	2420		

^a trs: solid–solid transition of non-specified nature. ^b fus: fusion. ^c fus(m): fusion (metastable). ^d Hot-stage polarizing microscopy. ^e Ferloni *et al.*'s⁽³⁾ information on $\text{CH}_3\text{CH}_2\text{CO}_2\text{K}$ solid-state transitions was further supported by subsequent (1979) X-ray diffractometric investigations^(9,10) carried out between 130 and 470 K in the same laboratory.

TABLE 2. Experimental heat capacities of lithium propanoate ($\text{CH}_3\text{CH}_2\text{CO}_2\text{Li}$) and potassium propanoate ($\text{CH}_3\text{CH}_2\text{CO}_2\text{K}$).^a ($R = 8.3144 \text{ J} \cdot \text{K}^{-1} \cdot \text{mol}^{-1}$)

T/K	$C_{p,m}/R$	T/K	$C_{p,m}/R$	T/K	$C_{p,m}/R$	T/K	$C_{p,m}/R$	T/K	$C_{p,m}/R$	T/K	$C_{p,m}/R$
Lithium propanoate											
(Results taken in Mark X cryostat)											
Crystal II											
Series I	343.90	17.613	159.33	9.811	236.17	12.954	86.49	6.108	21.98	0.850	
244.39	13.275		164.43	10.027	241.30	13.163	90.47	6.342	24.06	1.041	
250.88	13.560	Series II	169.54	10.247			94.47	6.564	26.41	1.265	
258.01	13.866	95.46	6.613	174.65	10.461	Series III	98.46	6.780	32.55	1.875	
265.15	14.163	99.25	6.821	179.75	10.674	237.13	12.982		35.89	2.208	
272.31	14.448	103.61	7.057	184.86	10.875	242.34	13.199	Series V	39.39	2.543	
279.47	14.763	108.63	7.332	189.98	11.098	247.53	13.403	8.48	0.060 ^b	42.96	2.870
286.63	15.075	113.65	7.596	195.11	11.304	252.67	13.629	9.11	0.117 ^b	46.60	3.194
293.80	15.391	118.69	7.865	200.24	11.519			10.01	0.103 ^b	50.29	3.511
300.96	15.698	123.73	8.124	205.37	11.719	Series IV		10.91	0.246 ^b	54.54	3.857
308.11	16.020	128.82	8.379	210.51	11.921	63.80	4.584	12.06	0.178	59.07	4.216
315.26	16.346	133.91	8.637	215.64	12.136	66.96	4.808	14.52	0.300	63.36	4.546
322.42	16.669	138.98	8.886	220.77	12.327	71.10	5.087	15.65	0.367	67.66	4.856
329.57	16.995	144.05	9.128	225.90	12.535	74.92	5.335	16.90	0.447	71.91	5.138
336.74	17.290	149.13	9.360	231.03	12.746	78.55	5.578	18.31	0.548		
		154.24	9.586			82.52	5.850	20.07	0.686		
(Results taken in Mark IX thermostat)											
Crystal II											
Series I	331.77	16.959	371.07	18.759	413.32	19.954	454.50	20.642	494.97	21.352	
310.08	16.241	340.43	17.639	381.37	19.129	423.63	20.135	464.62	20.844	505.07	21.544
317.41	16.658	350.61	17.968	392.74	19.467	433.94	20.351	474.74	20.983		
324.55	16.897	360.84	18.402	403.03	19.711	444.26	20.525	484.86	21.164		
Crystal I											
Series I	540.78	21.413	561.42	21.943	582.05	22.515					
530.85	21.291	551.10	21.709	571.74	22.218	592.37	22.774				
Potassium propanoate											
(Results taken in Mark X cryostat)											
Crystal III											
Series II	243.31	15.470	148.82	11.243	74.40	7.024	9.16	0.107	35.29	2.731	
170.80	12.151	247.90 ^c	15.700	153.93	11.464	77.83	7.308	10.19	0.145	38.75	3.179
175.66	12.354			159.05	11.669	81.53	7.609	11.35	0.196	42.50	3.653
181.81	12.618	Series III	164.15	11.895	85.51	7.922	12.65	0.268	46.66	4.180	
187.95	12.877	103.97	9.053	169.26	12.105	89.51	8.194	14.11	0.362	51.13	4.708
194.10	13.130	108.29	9.280	174.38	12.312	93.53	8.436	15.89	0.501	55.71	5.225
200.29	13.400	113.35	9.558	179.51	12.521	97.56	8.673	17.79	0.665	60.37	5.727
206.48	13.677	118.43	9.833			101.60	8.908	19.73	0.851	65.08	6.206
212.60	13.951	123.50	10.074	Series IV		105.65	9.136	21.95	1.084		
218.73	14.237	128.49	10.326	60.83	5.776			24.43	1.363	Series VI	
224.88	14.532	133.53	10.559	64.04	6.106	Series V		27.18	1.691	237.48	15.168 ^c
231.03	14.825	138.62	10.786	67.49	6.430	7.56	0.055 ^b	29.04	1.922		
237.17	15.141	143.72	11.012	70.95	6.733	8.32	0.079	32.16	2.320		

TABLE 2—continued

T/K	$C_{p,m}/R$	T/K	$C_{p,m}/R$	T/K	$C_{p,m}/R$	T/K	$C_{p,m}/R$	T/K	$C_{p,m}/R$	T/K	$C_{p,m}/R$
Transition (III → II) region											
Series II'	254.86	26.169	265.47	16.638	Series VI'	265.87	17.080	238.63	15.117		
250.91	16.156	255.36	27.244	269.39	16.431	287.07	16.877 ^c	271.06	16.646	245.78	15.464
252.85	17.436	255.88	26.219	273.85	16.444			276.84	16.640		
253.50	18.819	256.92	24.644	278.37	16.518	Series VII	283.09	16.762			
253.83	20.877	258.26	21.608	282.78	16.716	250.32	15.890	289.28	16.985		
254.13	22.672	259.41	19.183	287.09	16.867	253.82	16.565			Series IX ^d	
254.41	24.870	260.56	18.170			254.96	17.953	231.67	14.769		
		262.47	17.261			261.04	19.618				
Crystal II											
Series I	292.02	17.036 ^e	327.81	18.859	Series VIII	251.61	15.467 ^e	277.38	16.426 ^e		
271.42	16.172 ^e	299.19	17.365	334.97	19.376	238.56	14.943 ^e	257.98	15.708 ^e	284.06	16.705 ^e
277.68	16.414 ^e	306.36	17.668	342.07	20.133			264.41	15.952 ^e	290.74	16.964 ^e
284.86	16.742 ^e	317.08	18.215			Series X	270.90	16.202 ^e			
						245.01	15.216 ^e				

^a In chronological sequence by series, *i.e.* with increasing Roman numbers (I, II, II', II'', III, etc.) and within each series.

^b Not included in curve fit because of deviation from smooth curve.

^c Not employed for curve fit.

^d Crystal II partially converted into crystal III.

^e Crystal II in a metastable (undercooled) state.

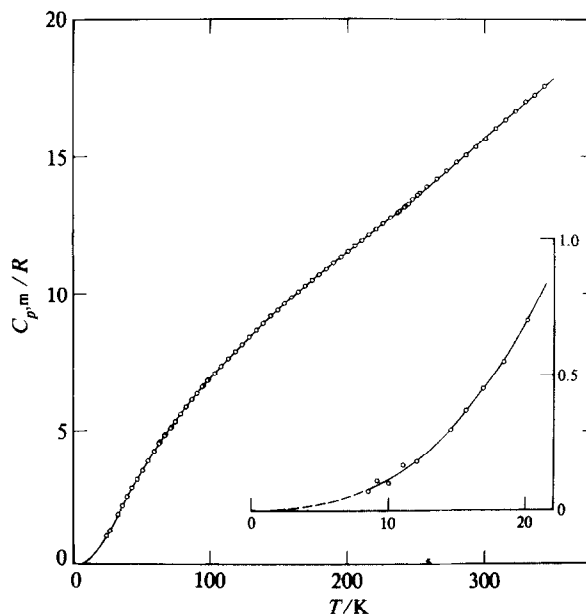


FIGURE 1. Heat capacities of lithium propanoate taken in the Mark X cryostat below 350 K.

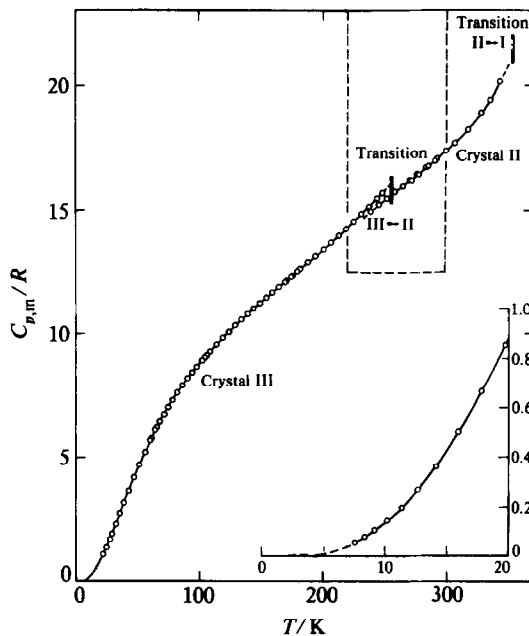


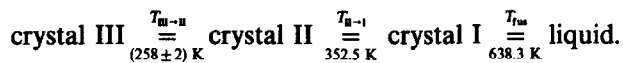
FIGURE 2. Heat capacities of potassium propanoate taken in the Mark X cryostat below 350 K. The interval between 220 and about 300 K (which includes the III \rightarrow II transition region) is magnified in figure 3.

in figures 2 and 3 for potassium propanoate. For a set of selected temperatures, smoothed $C_{p,m}/R$ values and the derived thermodynamic functions were calculated as described in reference 1 and are listed in table 3.

The molar heat capacities obtained in the Mark IX thermostat for lithium propanoate are tabulated also in table 2 and shown in figure 4.

POTASSIUM PROPANOATE CRYSTALLINE PHASES II AND III

D.s.c. allowed one of us⁽³⁾ to obtain evidence for the following phase relations in potassium propanoate:



Massarotti and Spinolo⁽¹⁰⁾ claimed on the basis of powder X-ray diffractometry that crystal I is orthorhombic and crystal II monoclinic, and that the latter exists in a metastable (undercooled) state to about 30 K below $T_{\text{III} \rightarrow \text{II}}$. Moreover, the structural differences between crystal III and crystal II—unambiguously proved by the recorded patterns—were so remarkable (although the indexing procedure was unsuccessful with crystal III) that a “true” (first-order) phase change is probably involved in the (III \rightarrow II) transformation. However, the present calorimetric results (compare figure 3) show that the transition is not isothermal.

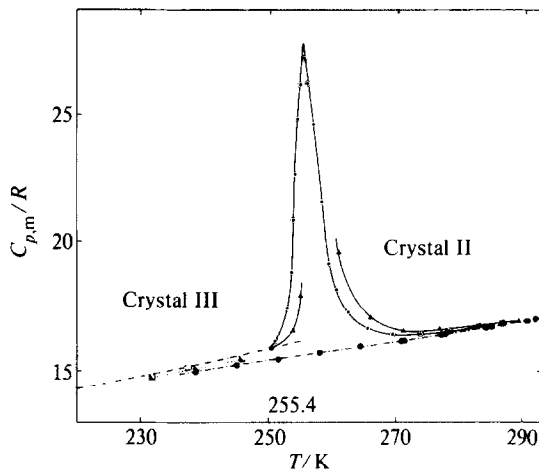


FIGURE 3. Heat capacities of potassium propanoate taken in the Mark X cryostat through the III \rightarrow II transition region. For further explanation see text.

The possibility that crystalline solids might undergo gradual phase transitions has been discussed by Allen and Eagles.⁽¹¹⁾ Their arguments were adopted, *e.g.* by Oetting and McDonald⁽¹²⁾ to classify the ($\alpha \rightarrow \beta$) transition of magnesium pyrophosphate as first-order, and it is to be stressed that the heat-capacity curve of this salt has features in the ($\alpha \rightarrow \beta$) transition region quite similar to those observed in the (III \rightarrow II) transformation range of potassium propanoate.

Massarotti and Spinolo's⁽¹⁰⁾ results as well as the shape of the heat-capacity curve suggest—even in the absence of supplementary information, *e.g.* on the pertinent volume change—that the $\text{CH}_3\text{CH}_2\text{CO}_2\text{K}$ (III \rightarrow II) transition is of first rather than

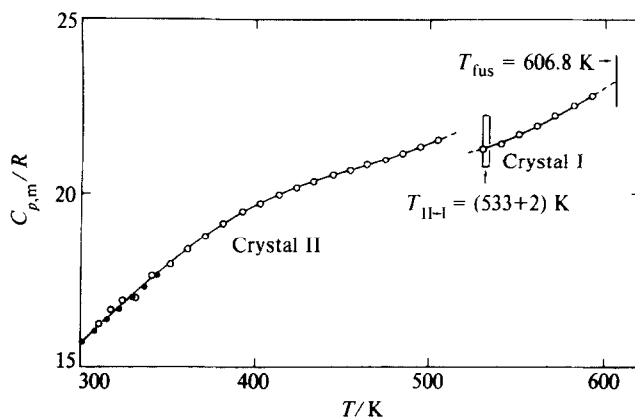


FIGURE 4. Heat capacities of lithium propanoate taken between 300 K and the melting temperature: ●, in the Mark X cryostat, and ○, in the Mark IX thermostat. The melting temperature and transition temperature are d.s.c. results from reference 3.

TABLE 3. Molar thermodynamic functions of propanoates ($R = 8.3144 \text{ J} \cdot \text{K}^{-1} \cdot \text{mol}^{-1}$)

$\frac{T}{\text{K}}$	$\frac{C_{p,m}}{R}$	$\frac{S_m^\circ(T) - S_m^\circ(0)}{R}$	$\frac{H_m^\circ(T) - H_m^\circ(0)}{R K}$	$\frac{G_m^\circ(T) - H_m^\circ(0)}{RT}$
Lithium propanoate				
Crystal II				
0	0.0	0.0	0.0	0.0
10	0.102	0.033	0.251	0.008
15	0.327	0.113	1.268	0.028
20	0.681	0.252	3.740	0.065
25	1.128	0.451	8.231	0.122
30	1.621	0.700	15.094	0.197
40	2.600	1.302	36.269	0.396
50	3.487	1.979	66.76	0.644
60	4.292	2.688	105.75	0.925
70	5.012	3.404	152.33	1.228
80	5.672	4.117	205.80	1.545
90	6.287	4.821	265.62	1.870
100	6.865	5.514	331.41	2.200
120	7.939	6.862	479.63	2.865
140	8.924	8.161	648.4	3.529
160	9.836	9.413	836.1	4.187
180	10.689	10.621	1041.4	4.835
200	11.504	11.790	1263.4	5.473
220	12.302	12.924	1501.5	6.099
240	13.105	14.028	1755.5	6.714
260	13.932	15.11	2025.9	7.318
280	14.788	16.17	2313.0	7.913
298.15	15.58	17.13	2588.6	8.445
300	15.67	17.22	2617.5	8.498
320	16.55	18.26	2939.7	9.076
350	17.97	19.81	3457.3	9.930
400	19.64	22.33	4400.9	11.323
450	20.60	24.70	5409	12.679
500	21.44	26.91	6459	13.993
514	(21.75) ^a	(27.51)	(6761)	(14.353)
Crystal I				
514	(21.17) ^a	(28.33)	(7186)	(14.353)
550	21.65	29.78	7954	15.32
600	22.94	31.72	9070	16.60
Potassium propanoate				
Crystal III				
0	0.0	0.0	0.0	0.0
10	0.135	0.046	0.341	0.012
15	0.430	0.150	1.679	0.038
20	0.877	0.332	4.891	0.087
25	1.429	0.585	10.620	0.161
30	2.044	0.900	19.284	0.257
40	3.339	1.665	46.190	0.510
50	4.577	2.545	85.85	0.828
60	5.690	3.480	137.31	1.191
70	6.655	4.431	199.16	1.586
80	7.482	5.375	269.95	2.001
90	8.195	6.299	348.42	2.427

TABLE 3—continued

$\frac{T}{K}$	$\frac{C_{p,m}}{R}$	$\frac{S_m^{\circ}(T) - S_m^{\circ}(0)}{R}$	$\frac{H_m^{\circ}(T) - H_m^{\circ}(0)}{R K}$	$\frac{G_m^{\circ}(T) - H_m^{\circ}(0)}{RT}$
100	8.821	7.195	433.56	2.860
120	9.902	8.902	621.1	3.726
140	10.849	10.501	828.8	4.581
160	11.716	12.007	1054.5	5.416
180	12.543	13.434	1297.2	6.228
200	13.384	14.799	1556.3	7.017
220	14.296	16.12	1833.0	7.785
240	15.29	17.40	2128.8	8.533
255	(16.10) ^a	(18.35)	(2364.1)	(9.082)
Crystal II				
255	(15.60) ^a	(18.60)	(2425.7)	(9.083)
260	15.78	18.90	2504.2	9.269
280	16.53	20.10	2827.1	9.999
298.15	17.30	21.16	3134.0	10.647
300	17.39	21.27	3166.1	10.712
320	18.37	22.42	3523.4	11.408
340	19.89	23.57	3904.2	12.089

^a At this transition temperature the values of the heat capacities are the extrapolated "lattice" values; the other thermodynamic properties are predicted on a presumably isothermal transition.

of higher order. The thermodynamic functions listed in table 3 were, therefore, calculated accordingly.

The temperature interval between 220 and about 300 K, which includes the (III → II) transition region, is magnified in figure 3. In order to fit polynomial 1 by least-squares through the experimental results taken on crystal II the points belonging to Series I, VIII, and X were employed (in figure 3 these points are represented by filled circles). Polynomial 2 was fitted through the results taken on crystal III, employing the points belonging to Series III, IV, and V along with those of Series II up to 243.31 K (in figure 3 these points are represented by open circles). In Series II, the point at 247.90 K (represented by an open square) still falls on the curve pertinent to polynomial 2, but the next (at 250.91 K) and the following ones (tabulated as Series II', and represented by circled dots) depart from it, going through a maximum ($T_{\max} = 255.4$ K) and finally joining polynomial 1. (In figure 3, the empty and filled squares represent heat capacities—belonging to different Series—relevant to crystal III and crystal II, which were not utilized for curve fitting.) The "transition region" thus apparently covers the interval between 249 and 293 K: consequently, results taken on crystal II below the latter temperature are to be attributed to a metastable (undercooled) state of this polymorph.

The area (in figure 3) whose upper boundary is the curve drawn through the circled dots and whose lower boundary is represented by the curve of polynomial 1 (---) from 293 down to 255.4 K, the extrapolated curve of polynomial 2 (---) from 249 up to 255.4 K, and a short vertical segment connecting the two curves at the latter temperature, was integrated graphically, and gave $\Delta_{\text{trs}} H_m/R = 62.3$ K. The rounded values $T_{\text{III} \rightarrow \text{II}} = (255 \pm 1)$ K and $\Delta_{\text{trs}} H_m/R = (62 \pm 1)$ K can be assumed as the (III → II) transition temperature and enthalpy increment. The previous d.s.c.

values:⁽³⁾ (258 ± 2) K and 40 K, respectively, can be favorably compared with them, although the agreement is not very close for the enthalpy increment.

It is to be stressed that the location of the transition is to some extent affected by the thermal history of the sample, in the sense that, after repeated cooling cycles, T_{trs} was found to be somewhat displaced towards the higher temperatures, as is apparent when the points of Series II' (circled dots in figure 3) are compared with those of Series VII (triangles). We recommend the T_{trs} value determined after the first deep cooling of the sample, *i.e.* (255 ± 1) K, as the correct one. In contrast, thermal history seems to have a minor influence on the heat capacities of the two phases involved.

In agreement with the findings by Massarotti and Spinolo,⁽¹⁰⁾ crystal II could be undercooled to about 235 K (compare Series VIII); cooling to about 230 K allowed us to observe a partial conversion to phase III (compare Series IX, whose points—represented by half-filled squares in figure 3—are intermediate between the curves of polynomials 1 and 2). Cooling to lower temperatures caused complete conversion to occur more quickly.

LITHIUM PROPANOATE IN THE SUPERAMBIENT REGION

Only one series of measurements was made in this region with the Mark IX thermostat; the silver calorimeter cracked during the first freezing of the molten salt. This prevented checking of the reproducibility of the heat capacities after fusion and subsequent cooling of the sample, and also the investigation of the (II \rightarrow I) transition and melting processes. The $C_{p,m}/R$ values taken on crystal II (in the upper part of its field of existence) and on crystal I are thus to be considered as exploratory, but nevertheless worthy of publication due to the (so far complete) lack of equilibrium values. The results are plotted in figure 4 along with the points taken at $T > 300$ K with the Mark X cryostat.

The agreement was satisfactory with the fusion temperature ($T_{\text{fus}} = 606.8$ K) obtained from d.s.c. records,⁽³⁾ while the transition (II \rightarrow I) was observed at a temperature $T_{\text{II} \rightarrow \text{I}} = (514 \pm 2)$ K remarkably lower than that, (533 ± 2) K, tabulated in reference 3. There is, however, no real discrepancy between the two findings, inasmuch as d.s.c. analysis allowed the authors⁽³⁾ to state that a powdered sample—like that employed in the present work—undergoes transition at a temperature at least 12 K lower than a previously melted sample—like that to which the $T_{\text{II} \rightarrow \text{I}}$ value tabulated in reference 3 actually refers. For the residual difference (about 7 K) allowance must be made for some sluggishness still exhibited by solid-state transitions of the propanoates, and for the fact that d.s.c. is a dynamic method of investigation.

COMPARISON AMONG LITHIUM, SODIUM, AND POTASSIUM PROPANOATES BELOW 300 K

The smoothed heat-capacity curves obtained for the three propanoates in the temperature range between the helium region and 273 K are compared in figure 5. At any given temperature, the heat capacity of potassium propanoate remains, as expected, larger than that of the sodium and lithium salts, whereas the $C_{p,m}/R$ curves for $\text{CH}_3\text{CH}_2\text{CO}_2\text{Na}$ and $\text{CH}_3\text{CH}_2\text{CO}_2\text{Li}$ cross at approximately 55 K. The

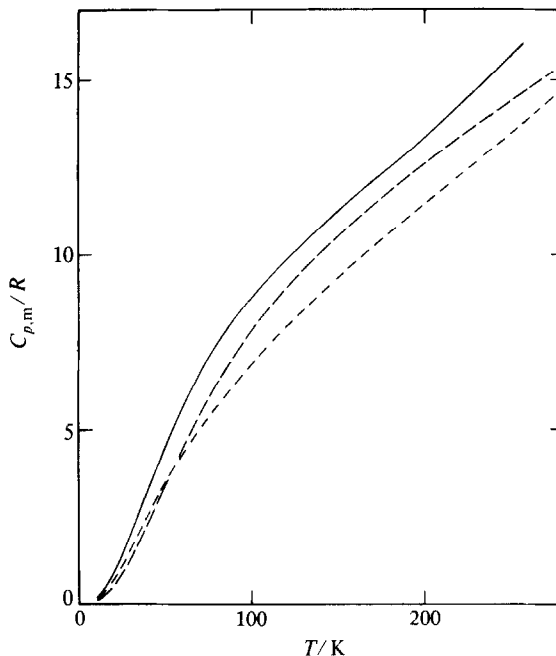


FIGURE 5. Comparison of $C_{p,m}/R$ taken in the low-temperature region for propanoates: ---, lithium; —, sodium; —, potassium.

reason for this peculiarity is so far not explained because structural information on lithium propanoate is not yet available.

We appreciate the assistance of William A. Plautz in devising computer programs and evaluation schemes to enhance the reliability of these experimental determinations and the resultant evaluated results. One of us (P.F.) gratefully acknowledges the financial support received by the National Science Foundation (U.S.A.) and by the Centro di Studio per la Termodinamica ed Elettrochimica dei Sistemi Salini Fusi e Solidi del C.N.R., Pavia (Italy).

REFERENCES

1. Franzosini, P.; Plautz, W. A.; Westrum, E. F., Jr. *J. Chem. Thermodynamics* **1983**, 15, 445.
2. Franzosini, P.; Westrum, E. F., Jr.; Plautz, W. A. *J. Chem. Thermodynamics* **1983**, 15, 609.
3. Ferloni, P.; Sanesi, M.; Franzosini, P. *Z. Naturforsch.* **1975**, 30a, 1447.
4. Sokolov, N. M. Summaries of Papers Presented at the 10th Scientific Conference of the Smolensk Medical Institute, **1956**. (This reference could not be consulted: it is, however, quoted as the pertinent primary source of information in subsequent papers from the same laboratory.)
5. Tsindrik, N. M.; Sokolov, N. M. *J. Gen. Chem. USSR* **1958**, 28, 1462.
6. Michels, H. J.; Ubbelohde, A. R. *J. Chem. Soc. Perkin II* **1972**, 1879.
7. Sokolov, N. M.; Minich, M. A. *Russ. J. Inorg. Chem.* **1961**, 6, 1293.
8. Baum, E.; Demus, D.; Sackmann, H. *Wiss. Z. Univ. Halle* **1970**, XIX, 37.
9. Cingolani, A.; Spinolo, G.; Sanesi, M. *Z. Naturforsch.* **1979**, 34a, 575.
10. Massarotti, V.; Spinolo, G. *J. Appl. Cryst.* **1980**, 13, 622.
11. Allen, J. W.; Eagles, D. M. *Physica* **1960**, 26, 492.
12. Oetting, F. L.; McDonald, R. A. *J. Phys. Chem.* **1963**, 67, 2737.